

NASA

Technical Memorandum 105600

AVSCOM

Technical Report 92-C-029

Effect of Out-of-Roundness on the Performance of a Diesel Engine Connecting-Rod Bearing

D. Vijayaraghavan
*Lewis Research Center
Cleveland, Ohio*

D.E. Brewe
*Propulsion Directorate
U.S. Army Aviation Systems Command
Lewis Research Center
Cleveland, Ohio*

and

T.G. Kieth, Jr.
*Ohio Aerospace Institute
Brook Park, Ohio
and University of Toledo
Toledo, Ohio*

Prepared for the
STLE/ASME Tribology Conference
sponsored by the ASME Journal of Tribology
St. Louis, Missouri, October 17-19, 1991

NASA

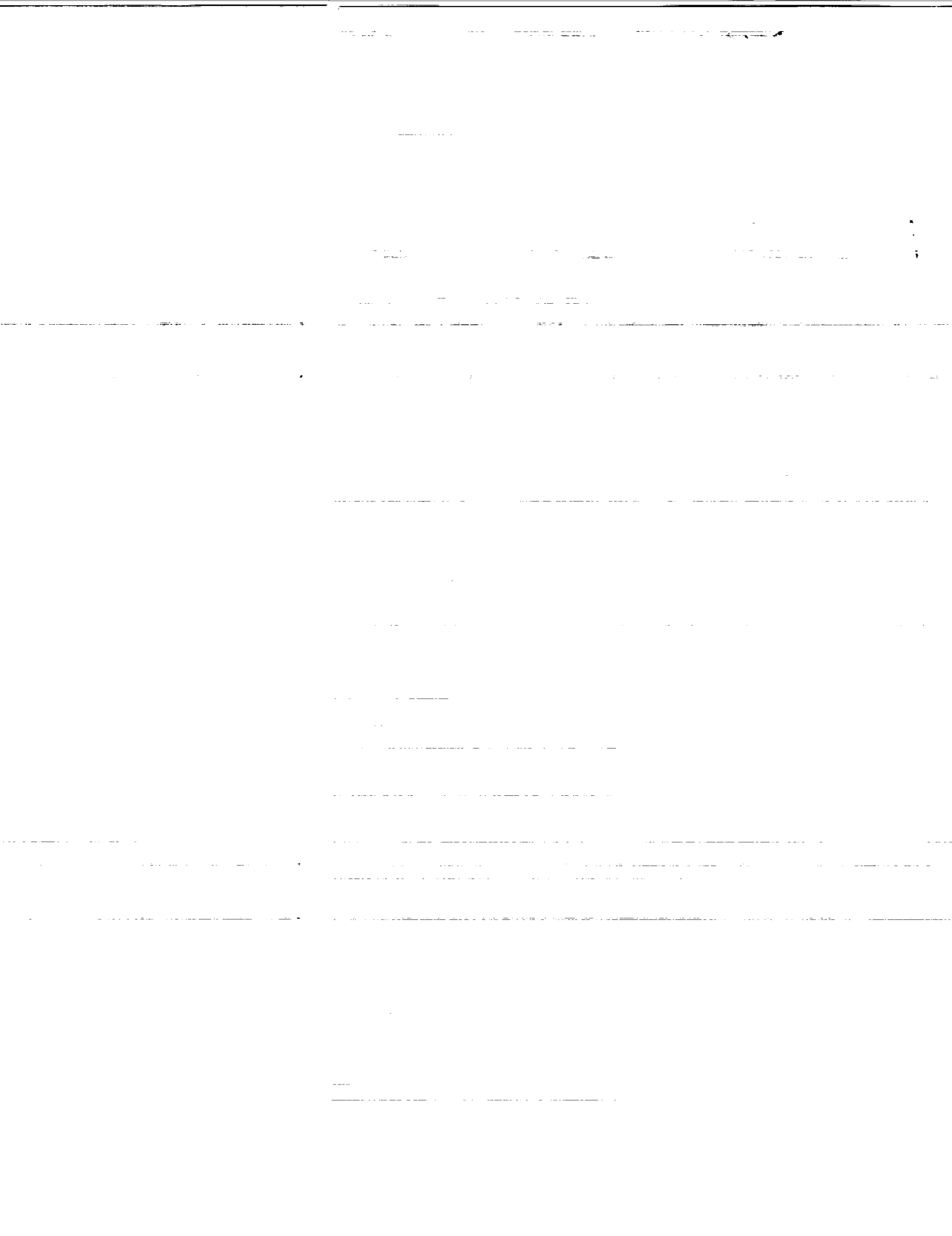


N92-31536

Unclass

G3/37 0116927

(NASA-TM-105600) EFFECT OF
OUT-OF-ROUNDNESS ON THE PERFORMANCE
OF A DIESEL ENGINE CONNECTING-ROD
BEARING (NASA) 19 p



Effect of Out-of-Roundness on the Performance of a Diesel Engine Connecting-Rod Bearing

D. Vijayaraghavan*

**National Aeronautics and Space Administration
Lewis Research Center
Cleveland, Ohio 44135**

D.E. Brewe

**Propulsion Directorate
U.S. Army Aviation Systems Command
Lewis Research Center
Cleveland, Ohio 44135**

T.G. Keith, Jr.

**Ohio Aerospace Institute
Brook Park, Ohio 44142
and
University of Toledo
Toledo, Ohio 43606**

SYNOPSIS

In this paper, the dynamic performance of the Ruston and Hornsby VEB diesel engine connecting-rod bearing with circular and out-of-round profiles is analyzed. The effect of cavitation is considered by using a cavitation algorithm, which mimics JFO boundary conditions. The effect of mass inertia is accounted for by solving coupled nonlinear equations of motion. The journal profiles considered are circular, elliptical, semi elliptical and three lobe epicycloid. The predicted journal trajectory and other performance parameters for one complete load cycle are presented for all of the out-of-round profiles and are also compared with the predictions for the circular bearing.

*National Research Council—NASA Research Associate at Lewis Research Center.

INTRODUCTION

The Ruston and Hornsby VEB diesel engine connecting-rod bearing is one of the most extensively analyzed bearings under dynamic loading conditions. This is perhaps due to the detailed compilation of all the theoretical predictions, experimental data and operational experiences for these bearings by Campbell et al (1967) and later by Martin (1983). Also, because of the complex loading pattern and the unsteady angular motion, these bearings pose an interesting problem to validate any numerical scheme. In addition, the specific loading of these bearings being large and operating minimum film thickness values being of the order of microns, realistic prediction of the performance of these bearings becomes very important.

In open literature, the theoretical methods of the prediction of the journal trajectory for the load cycle range from fast computational methods such as short bearing theory, mobility method (Booker, 1971), rapid curve fit method and a semi-analytical method (Ritchie, 1975), to more rigorous methods that use finite bearing analysis. Analyses have also been performed incorporating oil film history (Jones, 1983), mass effects (Holmes and Craven, 1971), oil feed features (Jones et al, 1982), thermal effects (Smith, 1983) and elastic effects (Fantino et al, 1983).

Jones (1983) utilized the concept of internodal flow by keeping track of the transport of oil within the control volume surrounding a node and by determining the degree of filling of the clearance space. However, the movement of the boundaries of the cavitated regions were not explicitly determined. When this approach of oil film history is applied to the analysis of the VEB big end bearing, the journal trajectory was similar in shape to previous predictions except for the small looping near the end of the load cycle (refer to Fig. 2e of Martin, 1983). However, a more dramatic conclusion was the prediction of a 2.3 micron minimum oil film thickness versus a value of 3.6 microns that was obtained without considering oil film history effects. The primary advantage in considering oil film history is the realistic determination of the oil flow. This, in turn, helps determine the operating temperature and the effective viscosity of the oil as well as improves estimates of the required pump capacity. The predicted flow averaged over the load cycle using oil film history compared favorably with experimental data. Dede, as reported by Martin (1983), analyzed the VEB big end bearing by taking into account the effective mass of the connecting-rod and concluded that the mass inertia effect might be significant only for main bearings adjacent to a fly wheel. However, some of the predicted journal trajectories utilizing this approach had smoother turns. For the finite bearing analysis, the predicted minimum film thickness was 4.45 microns. Martin and Booker (1966) studied the effects of changes in reciprocating and rotating masses and their relative proportions on the minimum film thickness of these bearings during the engine inertia loading.

Most of the analysis on the VEB big end bearings have been performed assuming that the bearing is perfectly circular. However, in practice, bearings are rarely circular. As pointed out by Campbell et al (1967) and Martin (1983), these bearings undergo considerable distortion under load. At times, the clearance space is similar to an elliptical bore bearing, with minimum film thickness occurring at two locations. Also, since the clearance of the bearing is considerably smaller than the radius, even small errors in manufacture or installation can cause considerable out-of-roundness. In addition, any debris in the oil and/or occasional rubbing of the journal on bearing surface over a long period of time can cause wear in the bearing surface, particularly in thin film regions. The connecting-rod bearing may also be designed with a noncircular geometry, perhaps,

to improve the performance or stability.

In this paper, the connecting-rod bearing of the Ruston and Hornsby VEB diesel engine is analyzed. A mass conservation algorithm (Vijayaraghavan and Keith, 1989) is used and is coupled with the nonlinear equations of motion that include the mass acceleration effect. The location of cavitation boundaries and the extent of the cavitated region are determined at every time step in the time march. In this sense, the oil film history is taken into consideration. The system of coupled linear ordinary differential equations of motion are solved using a fourth order Runge-Kutta method. The analysis is performed assuming that the journal and the bearing are rigid and the bearing has circular and out-of-round profiles. The elliptical bearing geometry can occur due to distortion and manufacturing / installation errors. A semi-elliptical geometry is modeled as an out-of-round bearing due to wear. While the above profiles pertain to bearings that are intended to be circular but operate with an out-of-roundness, the three lobed bearing model is considered as a noncircular bearing.

The authors (1991) analyzed the performance of the VEB big end bearing for circular, elliptical and worn profiles. The wear profile used in that study was based on the model developed by Dufrane et al (1983) for steam turbine journal bearings. In this model, it is assumed that the wear is caused by the imprint of the journal on the bearing surface and that the worn region spreads symmetrically due to the combination of abrasion and small lateral motion of the journal. The resulting worn arc has a radius larger than that of the journal. When this wear model was used in the analysis of the connecting-rod bearing, large fluctuations in pressure profile were observed during the computation. These fluctuations occurred whenever the journal moved into close proximity of the worn region edges. Nevertheless, this did not destabilize the computation as the overall film forces computed at such locations were comparable to those of the circular bearing. Subsequently, it was felt that for a bearing operating with such large lateral movement of the journal within a load cycle, a wear pattern with sharp corners at the extremes of the wear region would not be realistic and some smoothing of the wear profile would occur. Also, the wear model developed by Dufrane et al (1983) was for large steam turbine bearings operating at low speeds (10 rpm or less), when operating on turning gears. Under such conditions, the film thicknesses would be sufficiently low to allow wear by fine contaminants in the lubricant. For the present case, to model wear in connecting-rod bearings, it is assumed that the wear region has an elliptical profile without any sharp corners and the other half of the bearing will be circular. A three lobed bearing profile is also included in this present study to compare the performance of such profiles with that of circular bearings. The major axis of ellipse or the maximum depth of wear or the maximum clearance of the lobe are assumed to be in the region of occurrence of the minimum oil film thickness during the load cycle. Journal trajectories, the performance parameters and the pressure profiles are presented and compared with circular bearing results for the three configurations.

NOMENCLATURE

c	- Radial clearance (Minor clearance for out-of-round bearing)
c_M	- Major clearance
d_0	- Maximum wear depth
F_r	- Radial component of fluid film force
F_θ	- Circumferential component of fluid film force
h	- Film thickness
h	- Nondimensional film thickness [h/c]
L/D	- Bearing length to diameter ratio
M	- Equivalent mass of the connecting-rod
p	- Fluid pressure
p_c	- Cavitation pressure
p_a	- Ambient pressure
p_f	- Lubricant supply pressure
r	- Bearing radius
t	- Time
U	- Net surface velocity
W	- Applied load
x	- Co-ordinate axis in circumferential direction
z	- Co-ordinate axis in axial direction
α_b	- Angular position of maximum wear / major axis of ellipse
β	- Bulk modulus
δ_0	- Wear ratio (d_0/c)
ϵ	- Eccentricity ratio
ϵ_p	- Ellipticity ratio (c_M/c)
ϕ	- Attitude angle
ϕ_L	- Load vector angle
μ	- Fluid Viscosity
ρ	- Fluid density
ρ_c	- Fluid density at cavitation pressure
ω_j	- Angular velocity of the journal
ω_b	- Angular velocity of the bearing
ω_ϕ	- Angular velocity of the attitude angle
ω_L	- Angular velocity of the load
ψ	- Angular coordinate relative to line of centers

ANALYTICAL FORMULATION

Cavitation Algorithm

Elrod and Adams (1974) developed a single equation, which they termed the "universal equation", and which is applicable for the both full film and cavitated regions of the bearing. The derivation of this equation is based on the continuity of mass flow through the entire bearing. The unsteady, two-dimensional laminar form of the universal equation may be written as

$$\frac{\partial}{\partial t} (\rho_c h \theta) + \frac{\partial}{\partial x} \left(\frac{\rho_c U}{2} h \theta - \frac{\rho_c \beta}{12\mu} h^3 g \frac{\partial \theta}{\partial x} \right) + \frac{\partial}{\partial z} \left(-\frac{\rho_c \beta}{12\mu} h^3 g \frac{\partial \theta}{\partial z} \right) = 0 \quad (1)$$

where

$$\theta = \begin{cases} \rho/\rho_c & \text{in full film regions} \\ V_f/V_t & \text{in cavitated regions} \end{cases}$$

$$g = \begin{cases} 1 & \text{when } \theta \geq 1 \\ 0 & \text{when } \theta < 1 \end{cases}$$

$$\beta = \rho \frac{\partial p}{\partial \rho} = \theta \frac{\partial p}{\partial \theta} \text{ for } \theta \geq 1$$

In the above, V_t and V_f are the total clearance volume and the volume occupied by the fluid, respectively, g is the switch function and β is the bulk modulus of lubricant. In the full film region, $g=1$ and Eq.(1) reduces to a compressible form of the Reynolds equation. In the cavitated region, $g=0$, the pressure remains constant at the cavitation pressure and the flow is essentially driven by shear. The boundary conditions for film rupture and reformation are implicitly applied by enforcing conservation of mass flow across these boundaries.

Equations of Journal Motion

The journal motion, due to unbalanced fluid film forces, is described by the following scalar nonlinear equilibrium equations, written along and normal to the line of centers, respectively as

$$Mc \left[\frac{d^2 \epsilon}{dt^2} - \epsilon \left(\frac{d\phi}{dt} \right)^2 \right] = -F_r + W \cos \phi \quad (2)$$

$$Mc \left[\epsilon \frac{d^2 \phi}{dt^2} + 2 \left(\frac{d\phi}{dt} \right) \left(\frac{d\epsilon}{dt} \right) \right] = F_\theta - W \sin \phi \quad (3)$$

The fluid film forces F_r and F_θ are determined from integrating the instantaneous pressure

distribution, obtained by solving Eq.(1), using the following integrals

$$F_r = - \int_{-L/2}^{L/2} \int_0^{2\pi} p \cos \psi \, d\psi \, dz \quad (4)$$

$$F_\theta = \int_{-L/2}^{L/2} \int_0^{2\pi} p \sin \psi \, d\psi \, dz \quad (5)$$

By resolving the equations of motion along and normal to the line of centers, it is implicitly assumed that the co-ordinate system rotates along with the line of centers. Hence, any journal motion and load vector rotation are superimposed on the journal rotation. Therefore, the net surface velocity is computed from

$$U = r \left(\omega_j - \omega_b - 2\omega_L - 2 \frac{d\phi}{dt} \right) \quad (6)$$

Film Thickness

Since the angular frame of reference remains constant along the line of centers, the film thickness for the circular bearing is determined from

$$\bar{h} = 1 + \varepsilon \cos \psi \quad (7)$$

The film thickness for an elliptical bearing is adapted from Vaidyanathan and Keith (1989). For the physical arrangement shown in Fig.1, the film thickness equation for the elliptical bearing is written as

$$\bar{h} = 1 + \varepsilon \cos \psi + (\varepsilon_p - 1) \sin^2 \left[\psi + \left(\frac{\pi}{2} - \alpha_b + \phi + \phi_L \right) \right] \quad (8)$$

where α_b is the angular position of the major axis of the ellipse at any instant. In the case of a semi elliptical bearing, the film thickness for the elliptical region only can be obtained from Eq.(8). For the circular region of the bearing, Eq. (7) is used. The three lobed bearing profile is constructed based on the generation of an epicycloid profile by a particular point in a cylinder which is rolling on the outside of the circular bearing. The film thickness for this bearing is computed from

$$\bar{h} = 1 + \varepsilon \cos \psi + \delta_0 \left| \cos \left[\frac{N_L}{2} (\psi + \alpha_b - \phi - \phi_L) \right] \right| \quad (9)$$

where δ_0 is the maximum depth of the lobe, α_b is its angular position at any instant and N_L is the number of lobes.

Solution Procedure

The hydrodynamic 'universal equation', Eq.1, is discretized using the cavitation algorithm and solved using an approximate factorization numerical scheme which incorporates Newton iteration procedure for accurate transient solutions (Vijayaraghavan and Keith, 1990). The equations of motion are simultaneously solved using a fourth order Runge-Kutta method.

Since the circumferential groove extends through the entire circumference of the bearing, only one land of the bearing is analyzed. The axial edge of the bearing is maintained at the ambient pressure and the groove is maintained at the lubricant supply pressure. The cavitation pressure is taken to be absolute zero. The bearing data used in this analysis is given in Table 1. Initially the bearing is assumed to be filled with lubricant at the ambient pressure and released at an arbitrary location. For orientation of the out-of-roundness, α_b , is initially taken to be 45° . The analysis is performed by marching in time. Equation (1) is numerically solved to determine the current θ distribution based on the θ distribution from the previous time step and current eccentricity ratio. At every time step, the switch function distribution is updated. Newton iterations are performed, if necessary, only to reduce the residuals to a low level ($O(10^{-5})$). The force components F_r and F_θ are computed from the pressure profile. The applied load values and ω_L are also determined at every time step according to the polar load diagram. The power stroke of the piston is considered to be the start of the load cycle. Then the equations of motion, i.e., Eqs.(2) and (3), are solved for known values of M , c , W , F_r and F_θ and initial values of ϵ , ϕ , $d\epsilon/dt$ and $d\phi/dt$ to determine the new values of ϵ and ϕ . To begin the computation, $d\epsilon/dt$ and $d\phi/dt$ are taken to be zero. The procedure is repeated until the trajectory of the journal center repeats itself for every load cycle. For this bearing, within 180 degrees of crank revolution, the effects of the initial conditions disappear and the journal trajectory repeats itself for every load cycle. The trajectory of the journal, the forces developed by the fluid film, the net surface velocity, the minimum film thickness and the pressure distribution are recorded at specified time intervals. The code developed is vectorized and run on the CRAY XMP super computer.

RESULTS AND DISCUSSION

For the bearing profiles considered, the trajectories of the journal center relative to the connecting-rod axis are presented in Figs. 2a through 2d. The journal trajectory of the circular bearing resembles the trajectory predicted by Jones considering oil film history (Fig. 2e of Martin, 1983). However, the predicted minimum film thickness is 3.6 microns. The present prediction falls between the earlier predictions which considered either only the mass effects or only the oil film history.

In the case of out-of-round bearings, the clearance configuration varies with time due to the back and forth movement of the bearing. Hence, it is not possible to indicate the trajectory of the journal center and the clearance configuration for the entire load cycle without some co-ordinate transformation. In their previous work, the authors (1991) presented the journal trajectories as seen by a stationary observer and also indicated the clearance configuration corresponding to its orientation at the start of the cycle. In those plots, the journal trajectory appeared to touch or cross

the clearance configuration, although the minimum film thickness values determined at every time step, as shown in Fig.3, are well within limits. In this present effort, the trajectory plots are presented with respect to the major axis of the out-of-round profile. In other words, the clearance configuration is assumed to be fixed and the journal center location is transformed such that its orientation with respect to the major axis remains the same. To be consistent with this approach, such transformations have been performed for circular bearing also.

Figure 2b indicates the journal trajectory for the elliptical bearing. The trajectory conforms to the elliptical profile of the clearance configuration and the trajectory is within the clearance ellipse. Similarly, the journal trajectory for a semi-elliptical bearing, as shown in Fig. 2c, almost conforms to the clearance configuration. The journal center trajectory for the three lobed bearing is presented in Fig. 2d. In this case also, the journal trajectory is almost similar in shape to the clearance configuration. Some wiggles in predicted motion can be seen around the start as well as the end of the load cycle. Since the orientation of the maximum noncircularity is assumed to be at the locations where the eccentricity levels are large, it is expected that the changes in the journal trajectories compared to the circular bearing will be smaller at other orientations. The tendency of the journal motion to almost conform to the bearing clearance configuration may be due to the high specific loading and large operating eccentricity levels for the entire load cycle.

The minimum film thickness variations predicted for all the above cases are presented in Fig.3. The overall profiles of the minimum film thickness variation over the load cycle are very close to one another. This supports the observation (Campbell et al, 1967) that the absolute values of the minimum film thickness measured by a dynamic similarity machine for an operating distorted bearing and the theoretical predictions with the assumptions of a rigid, circular bearing have good correlation. In fact, they are within an order of magnitude of each other. However, there are deviations in the smallest minimum film thickness values and the location of such occurrences. The smallest minimum film thickness of 3.6 microns for the circular bearing occurs at a crank position of 270° from the top dead center (TDC). For the elliptical and semi-elliptical bearings, the smallest minimum film thickness values are nearly the same, but occurs at 260° from TDC. However, for the three lobed bearing, the smallest minimum film thickness value is dramatically lower (1.8 microns) and occurs later in the load cycle, at a crank position of 580° from the TDC. For these bearings generally operating at such low minimum film thickness values, even a small reduction in these values can substantially increase the risk of failure. It should also be pointed out that around the end of the load cycle the journal movement is rather large, resulting in drastic changes in minimum film thickness and attitude angle even for small changes in crank position, as attested by Figs. 2 and 3.

Similar to the fluctuations in the pressure profile predicted for the worn bearing whenever the journal is in the vicinity of the corners of the wear region, pressure fluctuations were observed for the three lobed bearing also. It is believed that these fluctuations are due to the convex profile of the bearing in these regions and the discretized film thickness profile is not able to accurately follow the actual film thickness profile, as the co-ordinate system rotates with the journal. Fortunately, these sharp fluctuations over a small region do not destabilize the computational procedure and the journal center trajectory is able to repeat itself for every load cycle. Hence, for the three lobed bearing, only cycle averaged performance parameters are provided in Table 2. From

Table 2, it can be readily seen that for the out-of-round bearings the maximum pressure values are larger by 5-30%, side leakage flow rates are larger by 20-50% and the power loss values are also slightly larger, when compared to circular bearings.

The predicted maximum pressure variations for the circular, elliptical and semi-elliptical bearings are shown in Fig. 4. The peak pressures for the out-of-round bearings are larger than those for the circular bearing. It is also interesting to note that the largest pressure developed by the film does not occur at the smallest film thickness, but rather, around the instant of peak firing force. The variations in side leakage flow rates for the complete bearing (both lands), corresponding to a lubricant supply pressure of 40 psi, are shown in Fig. 5. The profile is very similar to the values predicted with oil film history (Martin, 1983). The leakage rate for the noncircular bearings are larger than that of the circular bearing. The power loss during the load cycle as indicated in Fig. 6 is similar to the profile predicted by Martin (1985). The power loss for the elliptical bearings is similar to the values for circular bearings.

The pressure profiles and the cavitated regions undergo large variations during the load cycle. At times, two separate cavitated regions exist on either side of the pressure hump. Such occurrences are mainly due to the reversal of the velocity components. Figure 7 represents the pressure profiles for the various bearing profiles when the minimum film thickness is the smallest.

CONCLUSIONS

The Ruston and Hornsby VEB diesel engine connecting-rod bearing is analyzed considering cavitation and mass inertia effects. Three out-of-round bearing profiles, namely, elliptical, semi-elliptical and three lobed epicycloid are considered in the analysis. The orientation of the noncircular profiles are assumed to be at the region of maximum eccentricity values. The predicted journal center trajectories, minimum film thickness and other performance parameters for all the cases considered are presented and compared with the results for a circular bearing. Based on the analysis the following conclusions can be made:

1. For the circular bearing, the minimum film thickness as a function of crank angle is generally larger than the values predicted by Jones when oil film history was taken into account. This difference is believed to be due to the added consideration of mass inertia as well as oil film history in this analysis.

2. Out-of-roundness in bearing geometry causes:

- (a) reduced values of the smallest minimum film thickness and a shift in the crank position where such minimums occur (for three lobed bearing, the predicted smallest minimum film thickness is only 1.8 microns),

- (b) the motion of the journal, as observed from the rocking bearing, generally conforms to the bearing configuration and

- (c) an increase in the peak pressures, an increase in the average side leakage rate and almost the same average total power loss.

3. For this application, a circular bearing profile has better performance characteristics.

REFERENCES

- Booker, J.F., 1971, "Dynamically Loaded Journal Bearings: Numerical Application of the Mobility Method, *Transactions of the ASME, Journal of Lubrication Technology*, Vol 168, pp 168-176.
- Campbell, J., Love, P.P., Martin, F.A. and Rafique S.O., 1967, "Bearings for Reciprocating Machinery: A Review of the Present State of Theoretical, Experimental and Service Knowledge", *Proc. Inst. Mech. Engrs*, Vol 182, Part 3A, pp 51-74.
- Dufrane, K.F., Kannel, J.W. and McCloskey, T.H., 1983, "Wear of Steam Turbine Journal Bearings at Low Operating Speeds", *ASME Journal of Lubrication Technology*, Vol 105, pp 313-317.
- Elrod, Jr., H.G., 1981, "A Cavitation Algorithm", *ASME Journal of Lubrication Technology*, Vol 103, No. 3, pp 350-354.
- Elrod, Jr., H.G. and Adams, M.L., 1974 "A Computer Program for Cavitation and Starvation Problems", *Cavitation and Related Phenomena in Lubrication*, Mechanical Engineering Publications, New York, pp 37-41.
- Fantino, B., Frene, J. and Godet, M., 1983, "Dynamic Behavior of an Elastic Connecting-Rod Bearing: Theoretical Study", *Studies of Engine Bearing and Lubrication*, paper No 830307, pp 23-32; SAE/SP - 539.
- Holmes, R. and Craven, A.H., 1971, "The Influence of Crankshaft and Flywheel Mass on the Performance of Engine Main Bearings", *Proc. Inst. Mech. Engrs Trib Conv.*, Paper C63/71.
- Jones, G.J., 1983, "Crankshaft Bearings: Oil Film History", *Proc. 9th Leeds-Lyon Symposium on Tribology*, Leeds, Sep 1982, Tribology of Reciprocating Engines, Butterworths.
- Jones, G.J., Lee, C.S. and Martin, F.A., 1982, "Crank Shaft Bearings : Advances in Predictive Techniques Incorporating the Effects of Oil Holes and Groovings", *AE Tech Symposium*, Rugby, Warwickshire, U.K.
- Martin, F.A. and Booker, J.F., 1966, "Influence of Engine Inertia Forces on Minimum Film Thickness in Con-Rod Big-End Bearings", *Proc. Inst. Mech. Engrs*, Vol 181, Part 1, No. 3, pp 749-764.
- Martin, F.A., 1983, "Developments in Engine Bearing Design", *Tribology International*, Vol 16, No 3, pp 147-164.
- Martin, F.A., 1985 "Friction in Internal Combustion Engine Bearings", *Proc. Inst. Mech. Engrs*, Paper No. C67/85, pp 1-17, 1985.
- Ritchie, G.S., 1975, "The Prediction of Journal Loci in Dynamically Loaded Internal Combustion Engine Bearings", *Wear*, Vol 35, pp 291-297.
- Smith, E. H., 1983, "Temperature Variations in Crankshaft Bearings", *Proc. 9th Leeds-Lyon Symposium on Tribology*, Leeds, Sep 1982, Tribology of Reciprocating Engines, Butterworths.
- Vaidyanathan, K. and Keith, Jr., T.G., 1989, "Numerical Prediction of Cavitation in Noncircular Journal Bearings", *STLE Tribology Transactions*, Vol 32, No.2, pp 215 - 224.
- Vijayaraghavan, D. and Keith, Jr., T.G., 1989, "Development and Evaluation of a Cavitation Algorithm", *STLE Tribology Transactions*, Vol 32, No.2, pp 225 - 233.

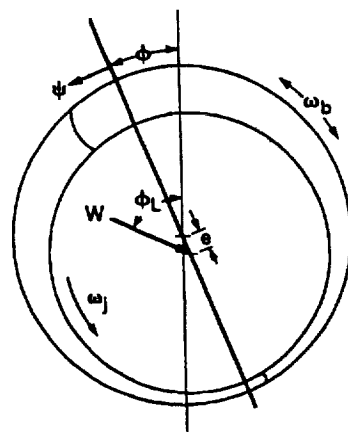
- Vijayaraghavan, D. and Keith, Jr. T.G., 1990, "An efficient, Robust and Time Accurate Numerical Procedure Applied to a Cavitation Algorithm", *ASME Journal of Tribology*, Vol 112, No. 1, pp 44 - 51.
- Vijayaraghavan, D., Brewe, D.E. and Keith, Jr., T.G., 1991, "Nonlinear Transient Analysis of a Diesel Engine Connecting-Rod Bearing with Circular and Noncircular Profiles", *Proceedings of 17th Leeds-Lyon Symposium on Tribology*, 1990, Leeds, Elsevier.

TABLE 1 : BEARING DATA

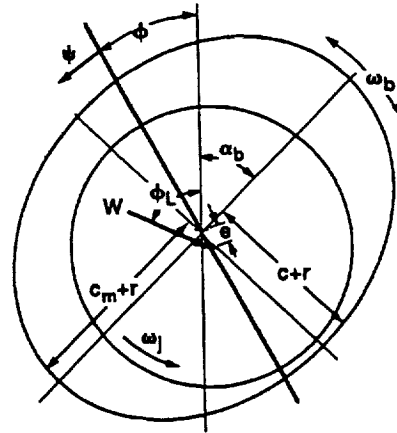
L/D		0.282
r	m	0.1
c	m	8.0×10^{-5}
P_a	N/m²	1.0133×10^5
P_f	N/m²	2.7579×10^5 (40 psi)
P_c	N/m²	0.0
M	Kg	54.0
β	N/m²	1.72×10^8
μ	Pa.s	0.015
ω	rad/s	62.84 (600 rpm)
ε_p		1.25
δ₀		0.25

TABLE 2 : COMPARISON OF PERFORMANCE PARAMETERS

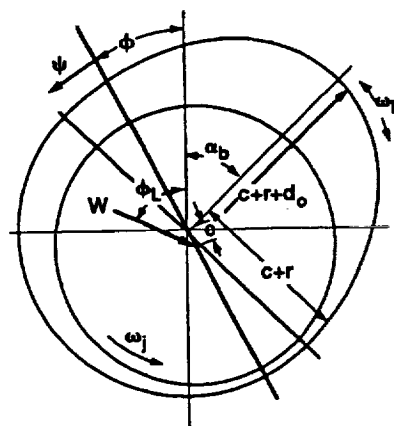
		Circular	Elliptical	Semi Elliptical	3 Lobe Epicycloid
Min. Film Thk	(μm)	3.6	3.52	3.51	1.8
Max. Pressure	(MPa)	35.64	37.25	37.14	46.97
Avg. Side Leak	(dm^3/s)	0.041	0.058	0.048	0.06
Avg. Power Loss	(kW)	1.269	1.348	1.317	1.286



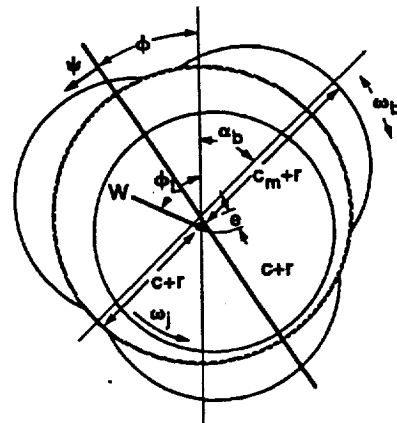
(a) Circular.



(b) Elliptical.

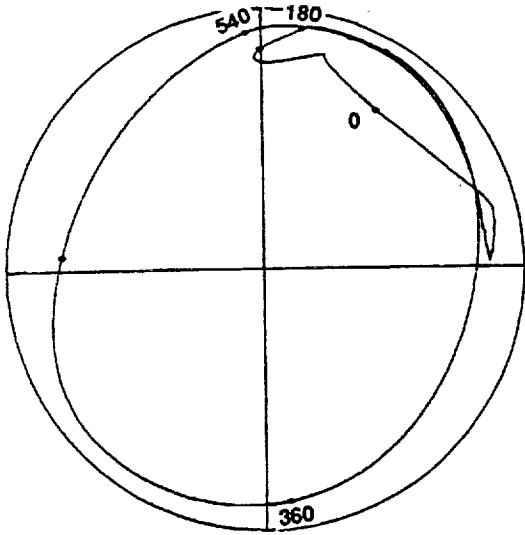


(c) Semi elliptical.

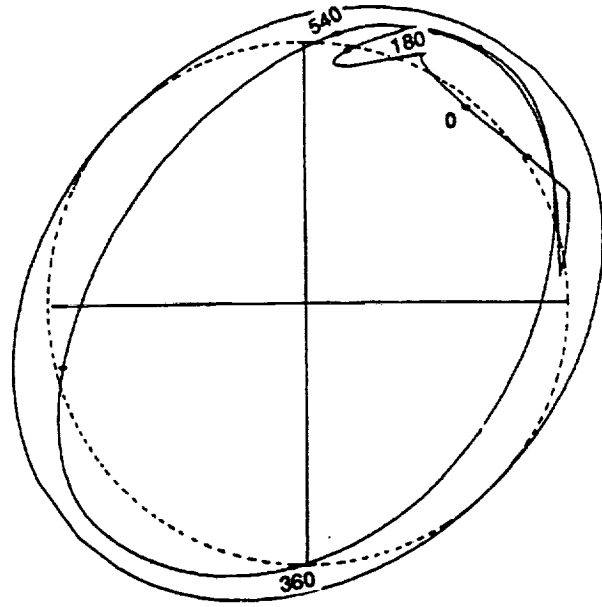


(d) 3 Lobe epicycloid.

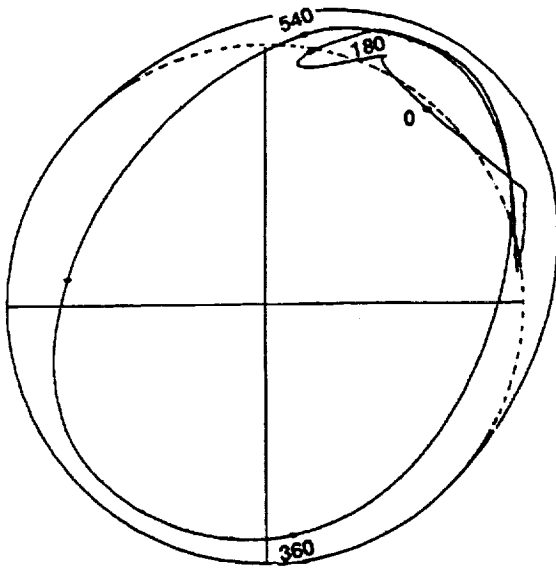
Figure 1.—Bearing geometry.



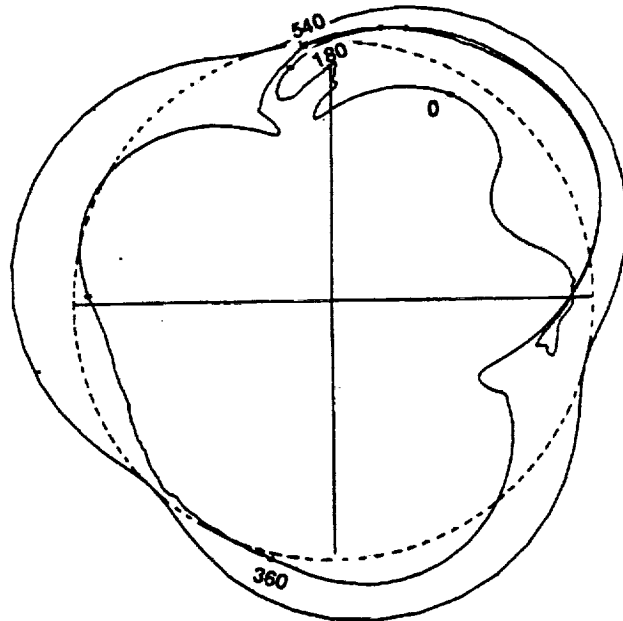
(a) Circular.



(b) Elliptical.



(c) Semi elliptical.



(d) 3 Lobe epicycloid.

Figure 2—Trajectory of journal center.

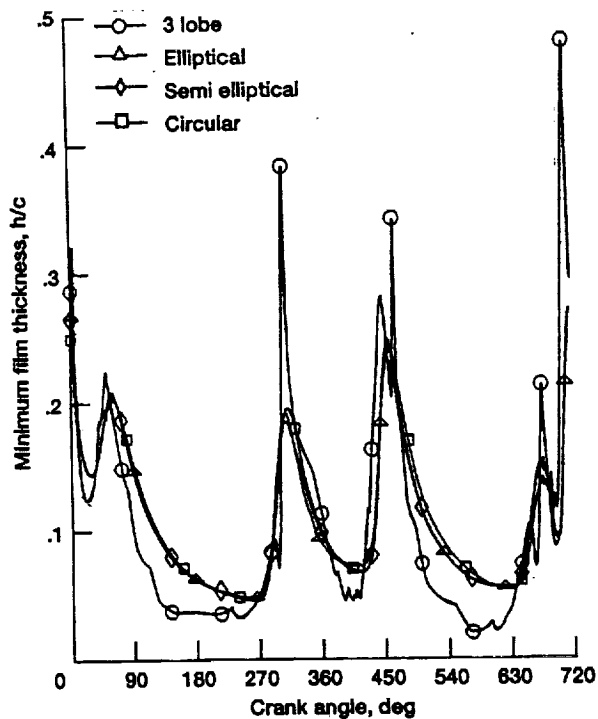


Figure 3.—Minimum film thickness.

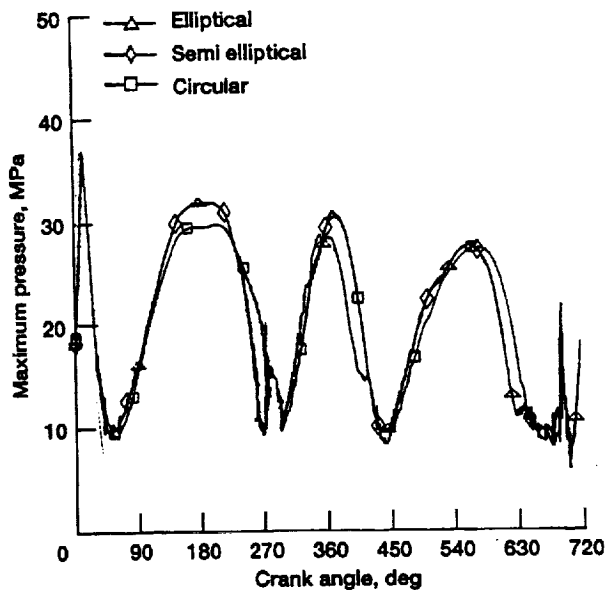


Figure 4.—Maximum pressure.

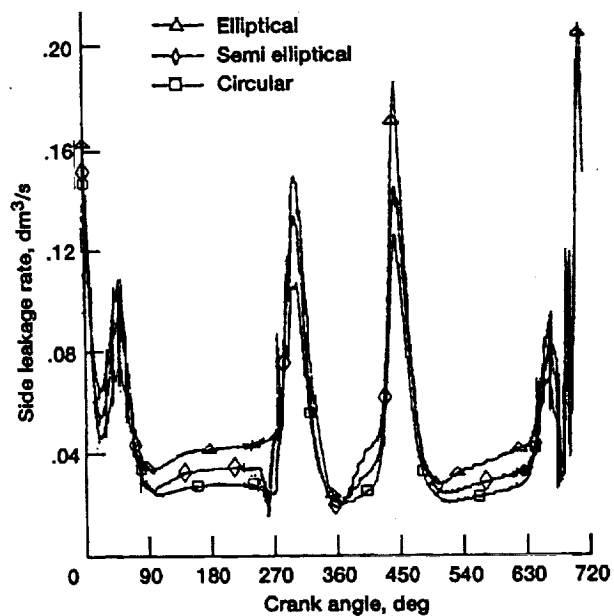


Figure 5.—Side leakage flow.

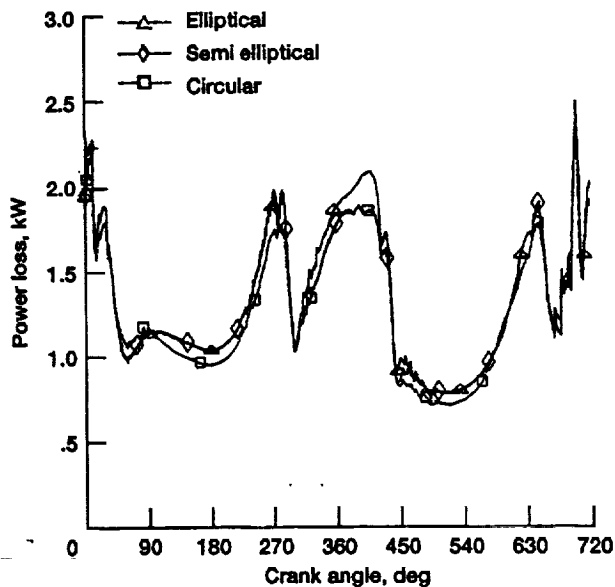
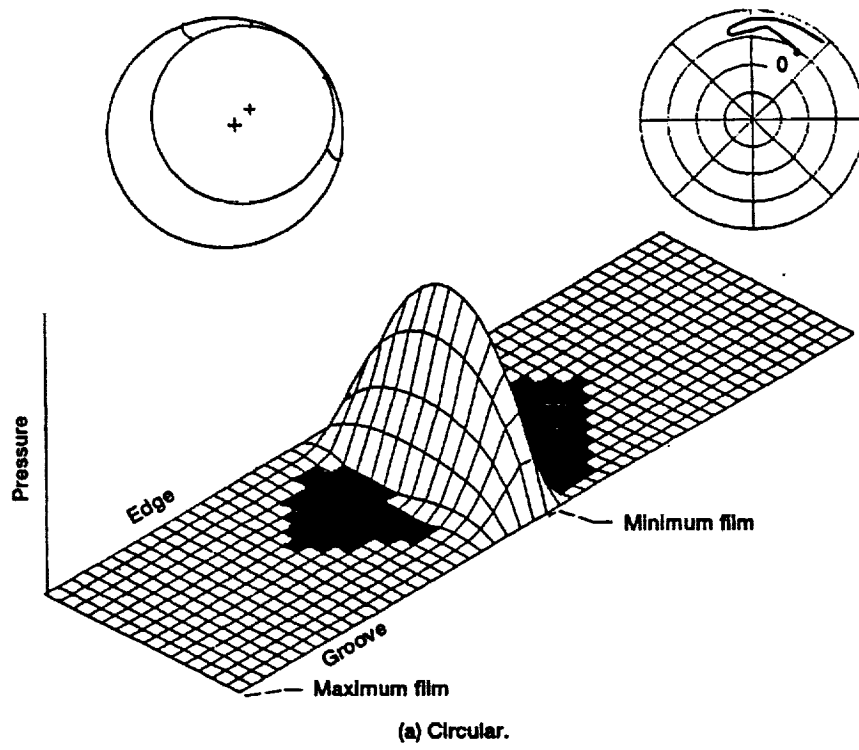


Figure 6.—Power loss.

$t = 73.2 \text{ ms}$



$t = 72.05 \text{ ms}$

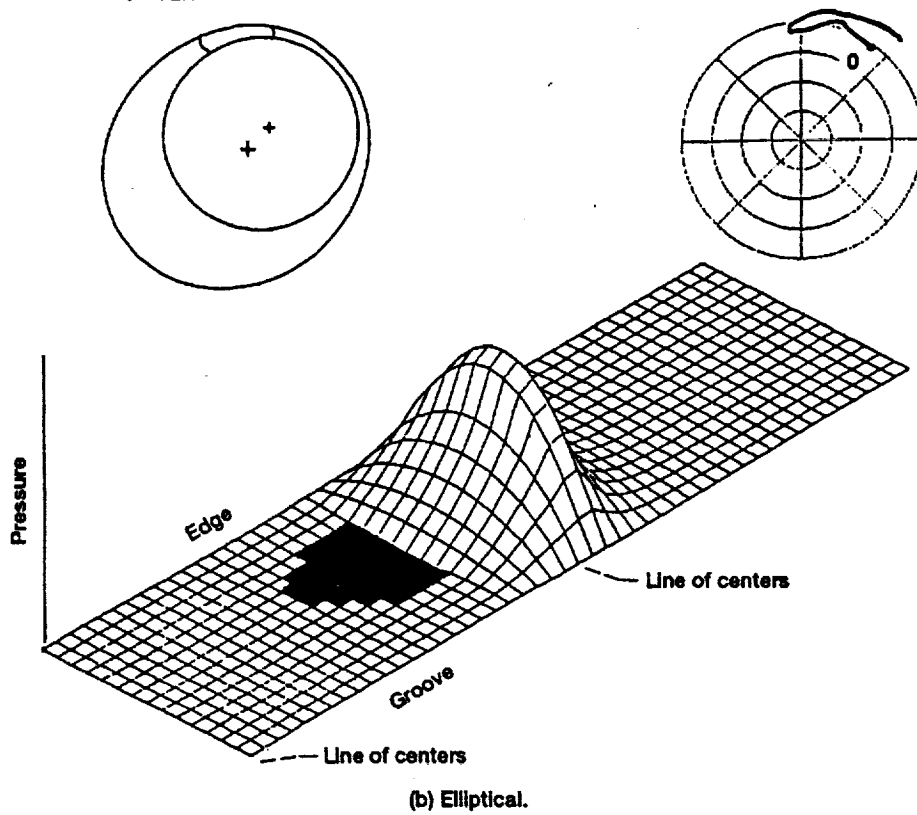


Figure 7.—Pressure profile at smallest minimum film thickness.

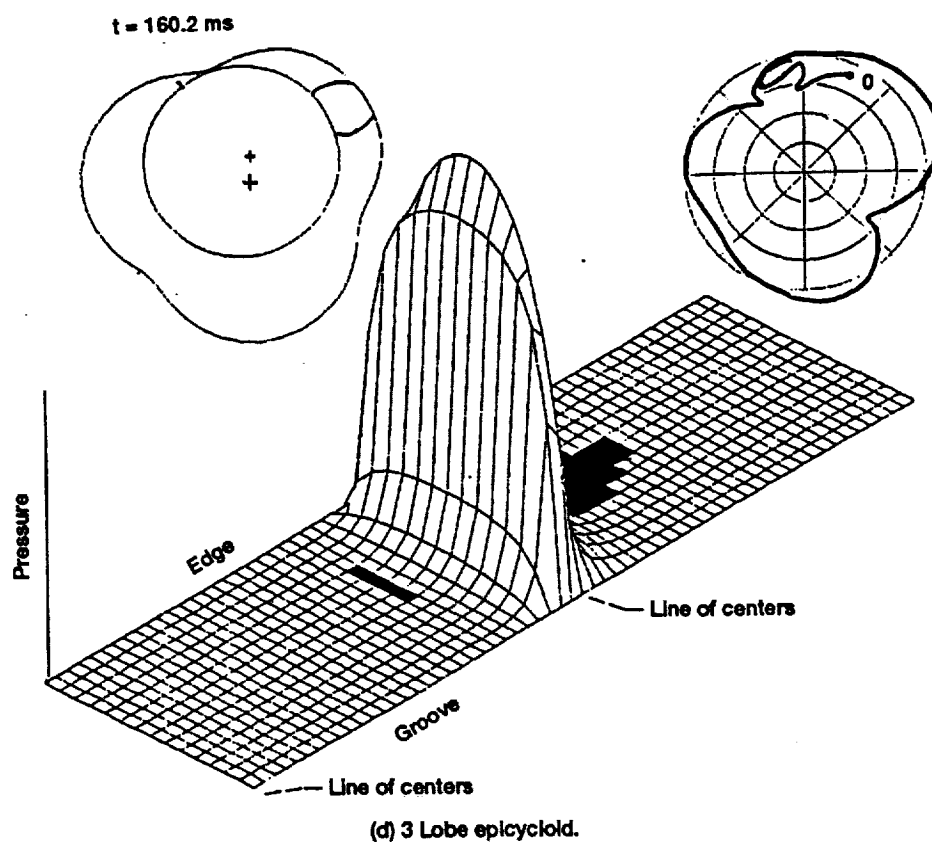
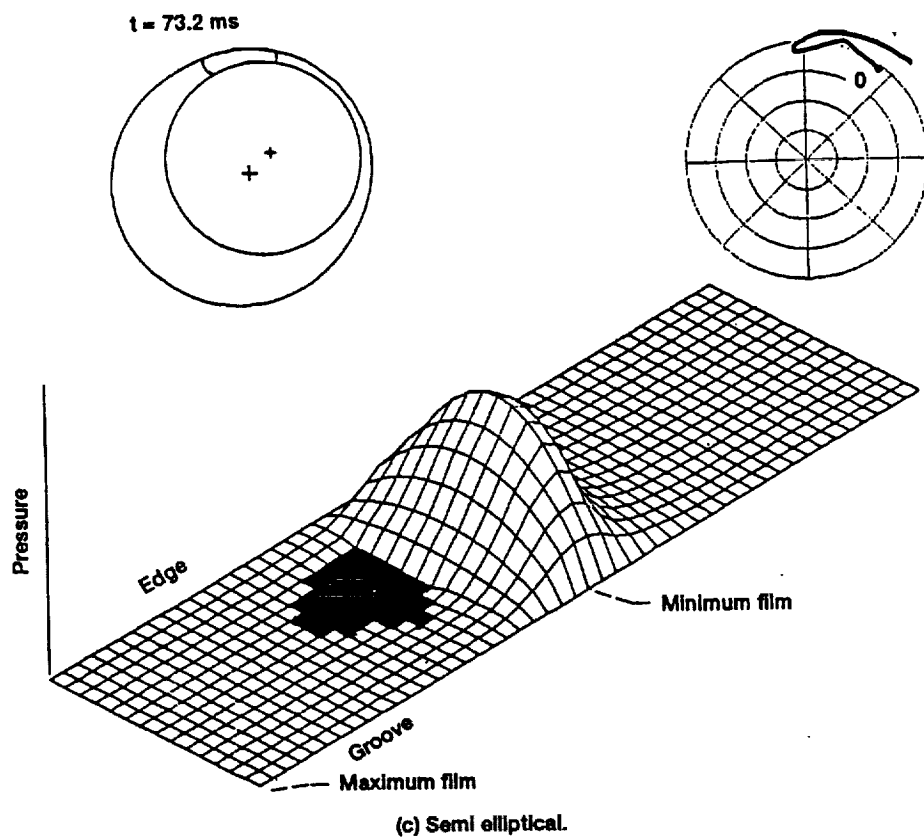


Figure 7.—Concluded.

REPORT DOCUMENTATION PAGE			Form Approved OMB No. 0704-0188	
Public reporting burden for this collection of information is estimated to average 1 hour per response, including the time for reviewing instructions, searching existing data sources, gathering and maintaining the data needed, and completing and reviewing the collection of information. Send comments regarding this burden estimate or any other aspect of this collection of information, including suggestions for reducing this burden, to Washington Headquarters Services, Directorate for Information Operations and Reports, 1215 Jefferson Davis Highway, Suite 1204, Arlington, VA 22202-4302, and to the Office of Management and Budget, Paperwork Reduction Project (0704-0188), Washington, DC 20503.				
1. AGENCY USE ONLY (Leave blank)	2. REPORT DATE October 1991	3. REPORT TYPE AND DATES COVERED Technical Memorandum		
4. TITLE AND SUBTITLE Effect of Out-of-Roundness on the Performance of a Diesel Engine Connecting-Rod Bearing		5. FUNDING NUMBERS WU-505-63-5A		
6. AUTHOR(S) D. Vijayaraghavan, D.E. Brewe, and T.G. Keith, Jr.				
7. PERFORMING ORGANIZATION NAME(S) AND ADDRESS(ES) NASA Lewis Research Center Cleveland, Ohio 44135-3191 and Propulsion Directorate U.S. Army Aviation Systems Command Cleveland, Ohio 44135-3191		8. PERFORMING ORGANIZATION REPORT NUMBER E-6863		
9. SPONSORING/MONITORING AGENCY NAMES(S) AND ADDRESS(ES) National Aeronautics and Space Administration Washington, D.C. 20546-0001 and U.S. Army Aviation Systems Command St. Louis, Mo. 63120-1798		10. SPONSORING/MONITORING AGENCY REPORT NUMBER NASA TM-105600 AVSCOM TR-92-029		
11. SUPPLEMENTARY NOTES Prepared for the STLE/ASME Tribology Conference sponsored by the ASME Journal of Tribology, St. Louis, Missouri, October 17-19, 1991. D. Vijayaraghavan, National Research Council - NASA Lewis Research Associate at Lewis Research Center; D.E. Brewe, Propulsion Directorate, U.S. Army Aviation System Command, and T.G. Keith, Jr., Ohio Aerospace Institute, 2101 Aerospace Parkway, Brook Park, Ohio 44142, and University of Toledo, Dept. of Mechanical Engineering, Toledo, Ohio 43606. Responsible person, D.E. Brewe, (216) 433-6067.				
12a. DISTRIBUTION/AVAILABILITY STATEMENT Unclassified - Unlimited Subject Category 37		12b. DISTRIBUTION CODE		
13. ABSTRACT (Maximum 200 words) In this paper, the dynamic performance of the Ruston and Hornsby VEB diesel engine connecting-rod bearing with circular and out-of-round profiles is analyzed. The effect of cavitation is considered by using a cavitation algorithm, which mimics JFO boundary conditions. The effect of mass inertia is accounted for by solving coupled nonlinear equations of motion. The journal profiles considered are circular, elliptical, semi elliptical and three lobe epicycloid. The predicted journal trajectory and other performance parameters for one complete load cycle are presented for all of the out-of-round profiles and are also compared with the predictions for the circular bearing.				
14. SUBJECT TERMS Journal bearing; Connecting-rod bearing; Cavitation; Diesel engine; Bearing geometry; Film thickness; Nonlinear equations; Fluid films		15. NUMBER OF PAGES 18		
		16. PRICE CODE A03		
17. SECURITY CLASSIFICATION OF REPORT Unclassified	18. SECURITY CLASSIFICATION OF THIS PAGE Unclassified	19. SECURITY CLASSIFICATION OF ABSTRACT Unclassified	20. LIMITATION OF ABSTRACT	